



Published in final edited form as:

*J Med Chem.* 2015 December 24; 58(24): 9562–9577. doi:10.1021/acs.jmedchem.5b01110.

## Molecular mechanism of action of triazolobenzodiazepinone agonists of the type 1 cholecystikinin receptor. Possible cooperativity across the receptor homo-dimeric complex

Aditya J. Desai<sup>1</sup>, Polo C.H. Lam<sup>2</sup>, Andrew Orry<sup>2</sup>, Ruben Abagyan<sup>3</sup>, Arthur Christopoulos<sup>4</sup>, Patrick M. Sexton<sup>4</sup>, and Laurence J. Miller<sup>1</sup>

<sup>1</sup>Department of Molecular Pharmacology and Experimental Therapeutics, Mayo Clinic, Scottsdale, AZ 85259

<sup>2</sup>Molsoft LLC, La Jolla, CA 92037

<sup>3</sup>Skaggs School of Pharmacy and Pharmaceutical Sciences, University of California, San Diego, La Jolla, CA 92037

<sup>4</sup>Department of Drug Discovery Biology, Monash Institute of Pharmaceutical Sciences and Department of Pharmacology, Monash University, Parkville, Victoria 3052, Australia

### Abstract

The type 1 cholecystikinin receptor (CCK1R) has multiple physiologic roles relating to nutrient homeostasis, including mediation of post-cibal satiety. This effect has been central in efforts to develop agonists of this receptor as part of a program to manage and/or prevent obesity. While a number of small molecule CCK1R agonists have been developed, none has yet been approved for clinical use, based on inadequate efficacy, side effects, or the potential for toxicity. Understanding the molecular details of docking and mechanism of action of these ligands can be helpful in the rational refinement and enhancement of small molecule drug candidates. In the current work, we have defined the mechanism of binding and activity of two triazolobenzodiazepinones, CE-326597 and PF-04756956, which are reported to be full agonist ligands. To achieve this, we utilized receptor binding with a series of allosteric and orthosteric radioligands at structurally-related CCK1R and CCK2R, as well as chimeric CCK1R/CCK2R constructs exchanging residues in the allosteric pocket, and assessment of biological activity. These triazolobenzodiazepinones docked within the intramembranous small molecule allosteric ligand pocket, with higher affinity binding to CCK2R than CCK1R, yet with biological activity exclusive to or greatly enhanced at CCK1R. These ligands exhibited cooperativity with benzodiazepine binding across the CCK1R homodimeric complex, resulting in their ability to inhibit only a fraction of the saturable binding of a benzodiazepine radioligand, unlike other small molecule antagonists and agonists of this receptor. This may contribute to the understanding of the unique short duration and reversible gallbladder contraction observed *in vivo* upon administration of these drugs.

A detailed understanding of the structural basis for activation of a receptor can contribute to the development of drugs with optimal properties for a particular application. The type 1 cholecystokinin (CCK) receptor (CCK1R) is a key mediator of post-cibal satiety and a potential target for drugs that may be useful to prevent and/or treat obesity<sup>1-4</sup>. However, while several small molecule allosteric agonists of this receptor have been developed, none has yet been approved for clinical use. These have had a variety of pharmacological properties, yet none to date has exhibited a clinical profile of adequate activity and absence of side effects or toxicity that might be compatible with long-term use by relatively healthy individuals.

The best understood docking of an allosteric full agonist of CCK1R at the present time is that of a 1,5-benzodiazepine<sup>5</sup>. It possesses an isopropyl group that acts as an agonist “trigger”<sup>6</sup> by interacting with a residue in transmembrane (TM) segment 7, Leu 7.39 (in nomenclature of Ballesteros and Weinstein<sup>7</sup>)<sup>5</sup>. While a series of reported agonists of this receptor are theoretically accommodated within this same pocket, with the pocket structure acting as a predictive discriminator between CCK1R agonists and antagonists<sup>5</sup>, detailed determination of binding poses has not yet been experimentally established for other members of this group. Such insights could be useful in refining drugs and could potentially contribute toward the development of new types of allosteric modulators that might possess unique clinical utility, such as positive allosteric modulators or allosteric agonists with varied degrees of intrinsic agonist activity.

In the current work, we have taken advantage of two triazolobenzodiazepinone agonists that have been reported to be full agonists of the CCK1R<sup>8,9</sup>. Their chemical structures are distinct from the 1,5-benzodiazepine that has had its docking studied in greatest detail previously<sup>5</sup>, and these ligands possess unique pharmacological properties worthy of further analysis. We have achieved these insights using receptor binding studies with a series of allosteric and orthosteric radioligands at the structurally-related human CCK1R and CCK2R, as well as a series of chimeric human CCK1R/CCK2R constructs exchanging residues that line the allosteric pocket, and biological activity studies at the same receptor constructs. These studies provide insights that refine our understanding of active conformations of this pocket and of the molecular mechanisms of inducing activity. The proposed poses of the ligands were further validated using site-directed receptor mutagenesis. Additionally, a unique feature of these allosteric agonists was their inability to fully inhibit the saturable binding of an allosteric antagonist radioligand. We show that this may be explained by cooperativity across the CCK1R homodimeric complex, a characteristic not shared by other existing allosteric ligands for this receptor that have been studied to date.

## RESULTS

### Pharmacologic characterization of CE-326597 and PF-04756956 at wild type CCK receptors

As previously reported<sup>8,9</sup>, both triazolobenzodiazepinones, CE-326597 and PF-04756956 (Fig. 1), were highly efficacious agonists, stimulating maximal intracellular calcium responses not statistically different from those elicited by CCK at the CCK1R (Fig. 2A). Concentration-response data demonstrated that PF-04756956 was a more potent agonist at

the CCK1R than CE-326597 ( $EC_{50}$  values (nM) of  $0.47 \pm 0.08$  for PF-04756956; and  $1.8 \pm 0.3$  for CE-326597) (Fig. 2A), and that PF-04756956 elicited no biological response at the CCK2R, while CE-326597 was a very weak partial agonist at that structurally-related receptor ( $EC_{50}$  of  $\sim 1\mu\text{M}$ ) (Fig. 2D).

Both CE-326597 and PF-04756956 bound to both CCK1R and CCK2R, as demonstrated by competition-binding studies with both a radiolabeled analogue of natural CCK and radiolabeled non-peptidyl benzodiazepines ( $^{125}\text{I}$ -BDZ-1 and  $^{125}\text{I}$ -BDZ-2) previously shown to bind to the intramembranous allosteric pocket (Fig. 2 B, C, E, F)<sup>10, 11</sup>.  $IC_{50}$  (nM) values of  $26.8 \pm 2.3$  and  $35.0 \pm 5.1$  were observed for these two ligands, respectively, for  $^{125}\text{I}$ -CCK binding to the CCK1R (Fig. 2B), while they inhibited only approximately 60% of saturable  $^{125}\text{I}$ -CCK binding to the CCK2R, with competition curves far to the right (Fig. 2E). Analysis of these data using a competitive binding model suggested low affinity binding to the receptors, with that for CCK1R higher than that for CCK2R (Table 1). We have, however, shown in our previous studies that the small molecule ligands of the CCK receptor have a distinct allosteric binding site within the intramembranous interhelical region<sup>5, 11, 12</sup>, which is different from the orthosteric binding site. For this reason, the data for the triazolobenzodiazepinone inhibition of  $^{125}\text{I}$ -CCK binding were also analyzed using an allosteric ternary complex model<sup>13</sup> to determine equilibrium constants ( $K_b$ ) and cooperativity constants ( $\alpha$ ) of modulators (Table 1). This analysis suggested lower  $K_b$  values for both compounds at CCK1R than at CCK2R, with values for  $\alpha$  at CCK1R not different from zero for either compound indicative of very high negative cooperativity that is indistinguishable from a competitive interaction, while both had relatively weaker negative binding cooperativity at the CCK2R. The binding selectivity was greater for PF-04756956 than for CE-326597.

To gain additional insights into the characteristics of the binding of the triazolobenzodiazepinones, their binding was also studied by competition for the previously described, selective benzodiazepine antagonist radioligands of the CCK1R and CCK2R,  $^{125}\text{I}$ -BDZ-1 and  $^{125}\text{I}$ -BDZ-2, respectively<sup>10, 11</sup>. Surprisingly, under the conditions of the binding assays, CE-326597 and PF-04756956 only partially inhibited the saturable binding of these radioligands to membranes expressing the wild-type CCK1R and CCK2R, with  $\sim 50\%$  and  $34\%$  inhibition, and with  $IC_{50}$  (nM) values of  $634 \pm 129$  and  $>1000$ , respectively, at the CCK1R WT; and  $IC_{50}$  values of  $175 \pm 47$  and  $>1000$ , respectively, at the CCK2R (Fig. 2 C, F). These data can be explained by two possibilities: (i) the triazolobenzodiazepinones may be acting allosterically relative to the BDZ ligands (and relative to the natural CCK peptide ligand), indicating the presence of another allosteric site on a monomeric receptor; or (ii) the triazolobenzodiazepinones may be acting at a site overlapping with the BDZ ligands, but across a dimeric receptor complex to explain cooperative behavior.

Because of these possibilities, these BDZ radioligand binding data were also fitted to both competitive and allosteric ternary complex models. Values are shown in Table 1. In contrast to the CCK radioligand binding data, these data suggest that the triazolobenzodiazepinones bind with higher affinities to CCK2R than to CCK1R. Despite the higher binding affinities

to CCK2R than to CCK1R, PF-04756956 possesses no agonist activity at all at CCK2R and CE-326597 is only a weak partial agonist at CCK2R (Fig. 2).

### CE-326597 and PF-04756956 function at CCK1R/CCK2R chimeras

In order to understand the mode of binding of these compounds at the CCK1R and the residues important for activation, we utilized a structure-activity approach using chimeric CCK1R/CCK2R constructs that exchanged the residues lining the allosteric pocket that are distinct in the two subtypes of CCK receptors (sequence alignment shown in Figure 3). This involved residues within the individual TM 2, 3, 6 and 7 segments of CCK1R exchanged with the respective corresponding residues of CCK2R. This approach used the same CHO cell lines expressing the CCK1R/CCK2R chimeras as had been utilized successfully in determining the molecular nature of binding of benzodiazepine antagonist<sup>11</sup> and agonist<sup>5</sup> ligands to the CCK1R. As noted previously<sup>11</sup>, levels of receptor expression for the CCK1R-based chimeric receptor-expressing cell lines were 3.1-fold (CCK1R TM2), 1.75-fold (CCK1R TM3), and 2.4-fold (CCK1R TM7) higher than WT, whereas there was no change with the CCK1R TM6 construct. In the case of the CCK2R-based chimeric receptor-expressing cell lines, the CCK2R TM6 and CCK2R TM7 constructs exhibited 0.4-fold and 0.5-fold expression (lower than) that of the CCK2R WT cell line.

The intracellular calcium stimulation studies provided insights into the relative importance of the regions and residues lining the allosteric ligand-binding pocket (Fig. 4 and Table 2). Because there were clear differences in the biological activity of these compounds at the CCK1R and the CCK2R, the chimeric constructs in which those residues lining this pocket that are different in the two related receptors were exchanged were particularly informative. For CE-326597, the unique residues in TM6 and TM7 were clearly the most important, with significant loss of function when these regions were replaced with those of CCK2R (CCK1R I6.51V, F6.52Y, and L7.39H) (Fig. 4 A, Table 2), while the converse constructs in which the CCK1R residues in these regions were inserted into CCK2R, there was clear gain of function (Fig. 4 B, Table 2). For PF-04756956, the same TM segments were key, although the degrees of loss of function were different between the two compounds (Fig. 4 C, D, Table 2). Of further interest, replacing TM2 and TM3 segments of CCK1R with those of CCK2R (CCK1R N2.61T, T3.28V, and T3.29S) resulted in enhanced responses, with the maximal responses greater than those observed in response to CCK. The major impact for CE-326597 was TM2, while the major impact for PF-04756956 was TM3, again suggesting compound-specific differences.

The binding data are summarized in Table 3. For CE-326597 (Fig. 5 A, B), there was clear loss of binding affinity with a right shift in the inhibition of binding of <sup>125</sup>I-BDZ-1 when TM7 was replaced with this segment of CCK2R, while the converse construct exhibited increase in binding affinity with a left shift. This is consistent with the impact on biological activity described above. Of particular note, the TM6 constructs that also exhibited complementary gain and loss of function in the biological activity studies, had no significant impact on the binding to these constructs. The TM3 and TM2 constructs that increased biological activity also exhibited left shifts in their binding of <sup>125</sup>I-BDZ-1. Similar effects were observed for the inhibition of binding of the CCK radioligand for the TM7 and the

TM2 constructs (Fig. 5 C, D), although quantitatively these shifts were different for the two radioligands.

For PF-04756956 (Fig. 6 A, B), there was also clear loss of binding affinity with a right shift in the inhibition of binding of  $^{125}\text{I}$ -BDZ-1 when TM7 was replaced with this segment of CCK2R, while the converse construct exhibited gain of binding affinity with a left shift. This is consistent with the impact on biological activity described above. Also here, the TM6 constructs that exhibited complementary gain and loss of function in the biological activity studies, had no significant impact on the binding of these constructs. The TM3 and TM2 constructs that increased biological activity also exhibited left shifts in their binding of  $^{125}\text{I}$ -BDZ-1. Similar effects were observed for the inhibition of binding of the CCK radioligand for the TM7 and the TM2 constructs (Fig. 6 C, D), although quantitatively these shifts were different for the two radioligands.

### Molecular models of docking of CE-326597 and PF-04756956 compounds

Molecular models were developed as described above. Figure 7 A, B and Figure 8 show the best poses determined for CE-326597 and PF-04756956 docked within the CCK1R. These compounds are predicted to utilize the same allosteric intramembranous interhelical pocket previously defined for GI181771X <sup>5</sup>, with contributions by TM2, 3, 6 and 7. Of note, these compounds occupied a larger volume than was previously defined by GI181771X. Both CE-326597 and PF-04756956 were predicted to dock with their C3-substituents oriented toward the extracellular region and the N1- and N5-benzodiazepine substituents pointing into the TM core bundle. For both of these compounds, the benzo ring was pointed toward TM3 and the phenyl group of the fused triazolobenzodiazepinone core was predicted to form an interaction with Asn 2.65, whereas the triazolo group was predicted to point toward the extracellular region between TM6 and TM7.

In contrast to GI181771X, the N1-benzyl group of the N1-isopropylbenzyl acetamide of CE-326597 was located deeper inside the pocket pointing toward the hydrophobic region between TM3 and TM6 and was predicted to make a limited interaction with Val 3.36 (Fig. 7 A). The N1-isopropyl group of this compound was situated similarly to that of GI181771X when docked, pointing toward the hydrophobic region of TM7, with an interaction with Leu 7.39 being predicted. Additionally, this group was predicted to be situated near residues Met 3.32 and Trp 6.48 as well. Similar to the determinant for biological activity of GI181771X <sup>5</sup>, Leu 7.39 was shown to be critical in the ligand structure-activity experiments in this study as well, further supporting the importance of this group in agonist activity <sup>5</sup>.

In the case of PF-04756956, the N1-dimethyl benzyl piperidine was predicted to dock quite differently than the N1-substituent of the GI181771X (Fig. 7 B). Of note, the N1-piperidine amide in PF-04756956 which is predicted to be the agonist “trigger” <sup>9</sup>, was postulated to point toward the hydrophobic pocket formed by TM6 and 7, forming interactions with Trp 6.48 and Leu 7.39. The C2-dimethyl phenyl substituent of the piperidine group was predicted to be accommodated in the pocket formed by TM2 and TM3 and to interact with Asn 2.61 of TM2. The 5-methyl group was capable of forming interactions with Thr 3.29 and Met 3.32 of TM3. Although the binding poses of CE-326597 and PF-04756956 were predicted to be accommodated in a similar pocket, the differences between the two are likely

marked by the position of the N1-benzyl (CE-326597) and the dimethyl benzyl at the C2 position of piperidine (PF-04756956) (Fig. 8). Whereas the N1-benzyl group of CE-326597 is buried deeper into the TM core facing down in the region between TM3 and TM6 (near Val 3.36), the dimethyl benzyl group of PF-04756956 is relatively more superficially located facing the TM2 and TM3 and does not make contact with Val 3.36 (Fig. 8).

### Characterization of receptor mutants involving residues predicted to be functionally important for triazolobenzodiazepinone activity

We attempted to validate the proposed molecular models using mutagenesis of some residues predicted by the models to be in spatial approximation with one or both of the triazolobenzodiazepinones, studying the impact on binding and biological activity of the compounds (Fig. 9 and Table 4). We prepared and studied alanine replacement mutants of Met 3.32, Val 3.36, and Trp 6.48 of the CCK1R. Each of these CCK1R mutants exhibited significant functional impact on triazolobenzodiazepinone binding and/or biological activity compared to the wild type CCK1R (Fig. 9, Table 4).

The potency of CE-326597 to stimulate intracellular calcium was reduced by a factor of 2 at the V3.36A mutant relative to its action at the wild type CCK1R, while that of PF-04756956 was reduced by a factor of 8 (Fig. 9 A, B). These effects could reflect the lower level of surface expression of this construct relative to wild type CCK1R (18 percent of that of wild type CCK1R) (Table 4). The models suggest that this residue may have more of an indirect role in agonist binding because CE-326597 is predicted to make a contact of less than 3 Å<sup>2</sup> and PF-04756956 does not dock deep enough to make any contact with this residue (Fig. 8).

The potency of CE-326597 to stimulate intracellular calcium was reduced by a factor of 56 at the W6.48A mutant relative to wild type CCK1R, while that of PF-04756956 was reduced by a factor of 12. Although this construct exhibited a lower level of surface expression than wild type CCK1R (16 percent of that of wild type CCK1R) (Table 4), there was no change in CCK-stimulated responses at this construct. This reduced potency of CE-326597 and PF-04756956 occurred in the setting of no change in the binding affinity of CE-326597 and an increase in affinity of PF-04756956 by a factor of 16 (Fig. 9 C, D, Table 4). The N1-benzyl ring of CE-326597 makes pi-pi interactions with this residue, which explains the bigger effect of this alanine mutation compared to PF-04756956, where the ring is directed away from TM6 (Fig. 8).

The largest differences were observed for M3.32A, which makes significant interaction contact area with CE-326597 and PF-04756956, 30 and 39 Å<sup>2</sup> respectively (Fig. 8). Neither triazolobenzodiazepinone exhibited any biological activity at this construct, in spite of high levels of surface expression and exhibiting very high binding affinity for CE-326597 and binding affinity not different from that for wild type CCK1R for PF-04756956 when using the <sup>125</sup>I-BDZ-1 radioligand (Fig. 9 A–D, Table 4). Of note, as a control to ensure normal biosynthesis and trafficking of this construct to the cell surface, CCK was shown to stimulate a full intracellular calcium response at the M3.32A mutant, with an EC<sub>50</sub> value of 0.13 ± 0.01 nM (Table 4).

## Possible impact of CCK1R dimerization on the binding characteristics of the triazolobenzodiazepinones

Because these data support substantial overlap in the site of docking of the triazolobenzodiazepinones with other small molecule allosteric ligands of CCK1R, the presence of a separate second allosteric ligand-binding site is an unlikely explanation for the inability of the triazolobenzodiazepinones to inhibit the saturable binding of the BDZ radioligand. We, therefore, experimentally evaluated the second stated possibility, that of impact of cooperativity across a CCK1R receptor homo-dimeric complex. Such a complex has been previously demonstrated to exist utilizing constructs of the rat CCK1R<sup>14</sup>, and key structural residues for dimerization occur within the lipid faces of TM6 and TM7<sup>14</sup>. In that work, this complex was shown to be substantially disrupted by a set of mutations along this interface, eliminating the receptor BRET signal without changing CCK binding or biological activity parameters<sup>14</sup>.

Therefore, BDZ radioligand binding was also performed using this mutant of the rat CCK1R (rCCK1R-Ala<sup>317,321,325</sup>)<sup>14</sup>. The BDZ-1 binding affinities were found to be similar in the wild type rat CCK1R and the mutant rat receptor (rCCK1R-Ala<sup>317,321,325</sup>), with pK<sub>i</sub> values of 9.55 ± 0.25 and 9.66 ± 0.09, respectively. Of note, the BDZ-1 binding affinity for the wild type rat CCK1R was significantly higher than that for the wild type human CCK1R (p < 0.05), with pK<sub>i</sub> values of 9.55 ± 0.25 and 8.38 ± 0.16, respectively. In these studies, the triazolobenzodiazepinones inhibited the binding of the BDZ radioligand to this CCK1R construct to a greater extent than they were able to at the wild type receptor (p < 0.05) (Fig. 10) (IC<sub>50</sub> values, nM, 76.54 ± 22.7 vs. 25.0 ± 3.13 for CE-326597; 168.3 ± 1.15 vs. 17.02 ± 1.49 for PF-04756956). Of note, the binding data for the Ala<sup>317,321,325</sup> mutant fit the two-site equation better than the one-site equation, whereas wild-type data best fit the one-site equation. These data are consistent with the triazolobenzodiazepinones exerting unique cooperativity across the CCK1R homodimeric complex. This property is not shared by the other small molecule antagonists and agonists previously studied<sup>5, 11</sup>.

## DISCUSSION

Cholecystokinin (CCK) is a gastrointestinal hormone released from enteroendocrine I cells in the proximal small intestine in response to protein and fat in the diet. The physiological relevance of CCK acting through the type 1 CCK receptor (CCK1R) is well established, with this hormone playing multiple roles involved in maintenance of nutritional homeostasis. These include stimulating pancreatic exocrine secretion and gallbladder contraction, modifying gastric emptying and gastrointestinal transit to optimize nutrient delivery for absorption, and stimulating post-cibal satiety<sup>3, 4, 15</sup>. The latter physiologic servomechanism is mediated by CCK action at CCK1Rs expressed on vagal afferent neurons<sup>2</sup>, contributing to maintenance of normal body weight. There is extensive evidence in preclinical and clinical studies documenting the ability of CCK to induce satiety and to reduce food intake, resulting in weight loss in animals and in humans<sup>1, 3, 16</sup>. Therefore, CCK1R, a class A Gq-coupled G protein-coupled receptor (GPCR), has been considered as an attractive drug target for agonists to induce satiety without adding caloric intake for the treatment of obesity. CCK1R agonists, including peptides<sup>1</sup>, peptoids<sup>17</sup>, and small

molecules (e.g. 1,5-benzodiazepine GI181771X<sup>18</sup>, imidazole carboxamide<sup>19</sup>, and thiazole SR 146131<sup>20</sup>) have been effective in reducing food intake in animals and humans, however none of these drugs have yet been approved for clinical use as a diet drug. This likely relates to on-target effects of the most potent agonists, including nausea, abdominal cramping, and diarrhea, and concern about potential trophic effects that could influence the development or progression of pancreatic cancer<sup>21, 22</sup>. There has been an extremely high bar for approval of such drugs, due to the very large potential market and the long duration of anticipated use by relatively healthy patients.

In order to elicit satiety, without prolonged agonist action at the CCK1R that might be associated with side effects and possible toxicity, there is a theoretical advantage to short duration action at the physiologically relevant target. In an attempt to achieve this, the Pfizer group chose to take advantage of physicochemical properties of the molecules in their discovery series, seeking an appropriate balance of solubility and membrane permeability to result in adequate exposure of active drug to enteric neurons, and rapid hepatic clearance to minimize systemic exposure<sup>8, 9</sup>. They were also interested in low biliary clearance to allow prompt gallbladder relaxation, as occurs physiologically. This was achieved by purposefully diverging from Lipinski's rule of five for bioavailable drugs, identifying candidates with higher molecular weight and lipophilicity than is typically targeted for drug development.

This series took advantage of the structure-activity relationships reported for development of a 1,5-benzodiazepine full agonist, GI181771X, which had identified the importance of the N1-isopropylanilidoacetamide for biological activity<sup>6</sup>. The fused triazolobenzodiazepinone core in this series was able to mimic the hydrogen bond acceptor properties of the carbonyl group at the C-4 position of the 1,5-benzodiazepine, while preserving binding and biological activity at the CCK1R. CE-326597 was the first candidate reported<sup>8</sup>, and PF-04756956 followed<sup>9</sup>. These replaced the isopropyl phenyl amide "trigger" present in GI181771X with either an isopropyl benzyl amide or a more divergent piperidine amide. CE-326597 also replaced the C3 urea substituent in GI181771X with a methyl indole, while PF-04756956 incorporated a methyl indazole. These molecules exhibited efficacy with no gastrointestinal side effects in pre-clinical rodent studies. A Phase 2 clinical trial of CE-326597 for 12 weeks in patients who were obese with type 2 diabetes mellitus did not achieve the desired endpoint<sup>8</sup>, and further clinical development was not pursued. While these ligands are not ideal drugs, they provide enough structural diversity from GI181771X and from each other to provide additional insights into the nature of allosteric agonist binding pose and into the determinants of activity. There are also some important and instructive lessons that were provided by the characterization and analysis of the binding data with these compounds.

Understanding of the structure of the intramembranous small molecule binding pocket within the CCK1R has been facilitated by the solution of crystal structures of more than 24 members of the class A GPCR family<sup>23</sup>. The helical bundle is the most conserved domain in these receptors, with substantial diversity in their loop and tail regions<sup>24</sup>. Indeed, earlier studies reported impact of mutations of residues lining this pocket on binding and/or function of various small molecule ligands of CCK1R, suggesting this as a site of their docking<sup>25-27</sup>. This was also subsequently directly demonstrated by photoaffinity labeling with a benzodiazepine ligand<sup>28</sup>. We have extensively characterized the conformations of



this pocket, as a site of docking various CCK1R antagonists<sup>11</sup> and agonists<sup>5</sup>, relying on a series of chimeric CCK1R/CCK2R constructs in which the residues lining this pocket that are distinct in these two receptors were exchanged. There are only six such residues within four transmembrane (TM) helices that are different in CCK1R and CCK2R<sup>11</sup>. In its inactive conformation occupied with a benzodiazepine antagonist, TM segments six and seven (residues 6.51, 6.52, and 7.39) are the most important for binding of BDZ-1, a CCK1R-selective ligand, whereas residues of TM segments two and seven (residues 2.61 and 7.39) are the most important for binding of BDZ-2, a CCK2R selective ligand<sup>11</sup>.

The active conformation of this pocket occupied with the benzodiazepine agonist, GI181771X, was distinct from the antagonist-occupied conformation, with a key role played by Leu 7.39 in interacting with the N1-isopropyl agonist “trigger” that has been proposed as being responsible for activation of the receptor<sup>5</sup>. It is not yet clear whether this mechanism will be relevant universally for activation of this receptor. Of note, in computational studies, this molecular model was predictive of binding of other small molecule agonists, effectively distinguishing these from a series of approved drug decoys, and even distinguishing CCK1R agonists from CCK1R antagonists<sup>5</sup>. We now have the opportunity to test this experimentally.

It is, perhaps, not surprising that the molecular basis of binding the natural orthosteric peptide ligand of CCK1R is less well defined. As for many peptide ligands, the extracellular loop and tail regions appear to play more important roles. With the structure of these less well defined than the helical bundle and given the inherent flexibility of linear peptide ligands, the techniques utilized become particularly important. There have been two contrasting docking poses of the natural orthosteric CCK peptide at the CCK1R that have been proposed<sup>27, 29, 30</sup>. One of these has been based predominantly on the functional impact of receptor mutagenesis and chimeric receptor constructs and has been interpreted that the carboxyl terminus of CCK occupies this same intrahelical pocket<sup>27, 31</sup>. The other has been based predominantly on spatial approximation constraints coming from the direct covalent labeling of receptor residues using intrinsic photoaffinity labeling with fully biologically active CCK analogues and has placed the carboxyl terminus of CCK above the lipid bilayer, adjacent to residue Trp<sup>39</sup> within the amino-terminal tail of CCK1R<sup>29</sup>, with the rest of the peptide residing along the external face of the lipid bilayer interacting with extracellular loop regions<sup>30, 32–35</sup>. Both models are believed to be compatible with extensive structure-activity data. The latter model has also been supported by fluorophore incorporation into the ligand for characterization of microenvironment<sup>36</sup> and fluorophore incorporation into ligand and receptor for relative distance determinations using fluorescence resonance energy transfer<sup>37</sup>.

One key difference in these models is particularly important for the current report, since the former would suggest that the small molecule ligands are occupying a part of the orthosteric ligand-docking pocket, while the latter suggests that the small molecules dock with a spatially distinct allosteric ligand-docking pocket. Classical pharmacological techniques have been utilized to distinguish these two possibilities<sup>12, 38</sup>. A key set of experiments was the ability of devazepide, a benzodiazepine antagonist, to elicit marked slowing of the dissociation of pre-bound CCK, an observation that is only possible through the binding of

the small molecule to a topographically distinct allosteric site within CCK1R simultaneous with CCK occupation. The cooperativity between orthosteric and allosteric ligands was also demonstrated and the kinetic parameters for the binding of each ligand were reported<sup>12</sup>. This is believed to best support the latter hypothesis, but more definitive evidence, such as a crystal structure for the CCK-occupied receptor, has not been reported.

To understand the binding mode of the triazolobenzodiazepinone agonists we have used analogous molecular modeling methods to those previously utilized to define the binding pose of GI181771X<sup>5</sup>. This approach has revealed similarities in the overall agonist binding pose, but differences in the orientation of some key groups. These observations can provide insights for rational efforts to develop or refine new drug leads. The benzo rings of the three agonists occupy the same general allosteric pocket, with their positions essentially identical among the models. The differences were most marked by the positions of the N1-benzyl group of CE-326597 and the dimethyl benzyl group at the C2 position of piperidine in PF-04756956, with the former buried deeper into the TM core facing the region between TM3 and TM6, while the latter is more superficially located facing TM2 and TM3.

The alanine-replacement mutation data for Trp 6.48, and Met 3.32 provide strong support for the models of CE-326597 and PF-04756956 bound to CCK1R. Met 3.32 makes significant contacts with both agonists, whereas in the case of CE-326597 additional pi-pi interactions between the N1 benzyl and Trp 6.48 are observed that can explain the very significant effect of the alanine mutation on biological responses to this compound.

In addition to the insights coming from the docking of these compounds, these experiments provide additional insights into the importance of the type of radioligand used in screening for and characterizing allosteric agonists. It is notable that the competition-binding approach yielded the most complete displacement using the orthosteric agonist peptide radioligand that binds to what we believe to represent a distinct site on the receptor, in contrast to the data with another allosteric radioligand that is an antagonist. Although the latter is believed to bind to the same pocket within the receptor, it binds to a distinct conformation of that pocket. Typically, however, we expect the conformations of a given receptor binding pocket to interconvert, particularly within the time frame necessary to achieve binding equilibrium. Binding conditions were carefully assessed in the current work and found to be adequate to reach equilibrium. However, it was clear that the triazolobenzodiazepinones were not able to fully inhibit the binding of the BDZ radioligand. This is in clear contrast with the behavior of other small molecule ligands that represent both antagonists<sup>11</sup> and agonists of this receptor<sup>5</sup>.

Two possible explanations were identified for this behavior: (i) the triazolobenzodiazepinones may be acting allosterically relative to the BDZ ligands (as well as relative to the natural CCK peptide ligands), indicating the presence of another allosteric site; or (ii) the triazolobenzodiazepinones may be acting at a site overlapping with the BDZ ligands, but across a dimeric receptor complex to explain cooperative behavior. Strong data are presented to make the first possibility unlikely. The docking experiments show the triazolobenzodiazepinones to occupy the same space high in the intrahelical bundle that

BDZ ligands occupy. This is further supported by directed receptor mutagenesis to test this prediction.

The observation of greater competitive inhibition of BDZ radioligand binding to a CCK1R mutant previously shown to disrupt receptor oligomerization<sup>14</sup> than to wild type CCK1R makes cooperativity across the receptor oligomeric complex a likely explanation for the observed binding events. This property of the triazolobenzodiazepinones is distinct from other small molecule allosteric antagonists and agonists studied similarly<sup>5, 11</sup>. The analysis of the triazolobenzodiazepinone inhibition of the BDZ radioligand binding to CCK1R reveals positive cooperativity, suggesting that the triazolobenzodiazepinone binding to one receptor protomer enhances the binding of the BDZ to the second protomer, and reduces the ability of the triazolobenzodiazepinones to displace it. This is the first significant functional effect of the dimerization of CCK1R that has been recognized to date<sup>14</sup>, providing potential pharmacological, if not physiological importance of this complex. It is also possible that the short duration of action and reversibility of the triazolobenzodiazepinone effect on gallbladder contraction<sup>8, 9</sup> is contributed to by this limited distribution of the binding sites of these unique ligands.

## EXPERIMENTAL PROCEDURES

### Materials

Ham's F-12 medium, OptiMEM medium, L-glutamine, Lipofectamine™ LTX and PLUS™ reagents were from Invitrogen (Carlsbad, CA). Quest Fluo-8-AM™ was from AAT Bioquest Inc. (Sunnyvale, CA). Fetal Clone II tissue culture medium supplement was from Hyclone laboratories (Logan, UT). Microscint™, Unifilter-96 well microplates with bonded GF/B filters were from PerkinElmer Life and Analytical Sciences (Shallon, CT). Costar 96-well V bottom assay plates and the black assay plates with clear bottoms were from Corning (Corning, NY). All other reagents were analytical grade.

### Ligands

The triazolobenzodiazepinone compounds, CE-326597 (N-benzyl-2-[(4S)-4-(1H-indol-3-ylmethyl)-5-oxo-1-phenyl-4,5-dihydro-6H-[1,2,4]triazolo[4,3-a][1,5]benzodiazepin-6-yl]-N-isopropylacetamide, also known as PF-00990631)<sup>8</sup> and PF-04756956 ((4S)-6-{2-[(2R)-2-(3,5-dimethylbenzyl)piperidin-1-yl]-2-oxoethyl}-4-(1H-indazol-3-ylmethyl)-1-phenyl-4H-[1,2,4]triazolo[4,3-a][1,5]benzodiazepin-5(6H)-one)<sup>9</sup>, were provided by Dr. Kimberly O. Cameron from Pfizer Global Research and Development, Groton, CT (structures shown in Fig. 1). Both compounds were evaluated by reversed-phase HPLC with UV detection at 215 nm, and were found to be greater than 95 percent pure. These ligands have been reported to act as full agonists at the CCK1R<sup>8, 9</sup>. Cholecystokinin octapeptide (CCK-26-33, based on the numbering of CCK-33; also known as CCK-8) was purchased from Peninsula Laboratories (Belmont, CA). The benzodiazepine ligands for the type 1 (BDZ-1, (S)-1-(3-iodophenyl)-3-(1-methyl-2-oxo-5-phenyl-2,3-dihydro-1H-endo[e][1,4]diazepin-3-yl)urea)<sup>10</sup> and type 2 (BDZ-2, (R)-1-(3-iodophenyl)-3-(1-methyl-2-oxo-5-phenyl-2,3-dihydro-1H-benzo[e][1,4]diazepin-3-yl)urea)<sup>10</sup> CCK receptors were kindly provided by Professor P.S. Portoghese of the University of Minnesota. Radioiodinated forms of these ligands were

prepared by oxidative radioiodination using the solid-phase oxidant, iodobeads (Pearce, Rockford, IL), with purification of the product to homogeneity on reversed-phase HPLC. The CCK-like radioactive tracer,  $^{125}\text{I}$ -D-Tyr-Gly-[(Nle<sup>28,31</sup>)CCK-26-33] ( $^{125}\text{I}$ -CCK), was prepared using similar oxidative radioiodination and HPLC purification techniques<sup>39</sup>. All radioligands were purified to homogeneity, yielding products with specific radioactivities of approximately 2000 Ci/mmol<sup>10</sup>.

### CCK receptor constructs and cell lines

Previously reported and characterized Chinese hamster ovary (CHO) cell lines stably expressing a series of CCK receptor constructs were used for this study (all of these were human receptors, unless specifically noted)<sup>5, 11</sup>. The new human CCK1R mutants used in this study included site mutants, N2.65A, M3.32A, V3.36A, and W6.48A, which were created by introducing single point mutations in the CCK1R WT construct in the pcDNA<sup>TM</sup>5/FRT vector by mutagenesis using the QuickChange<sup>TM</sup> kit (Stratagene, La Jolla, CA). All constructs were verified by direct DNA sequencing. Cell lines stably expressing these constructs were prepared in CHO cells, as previously described<sup>11</sup>. The cell lines were maintained in Ham's F-12 medium supplemented with 5% Fetal Clone II in a humidified environment containing 5% carbon dioxide, and were passaged approximately two times per week. A mutant of the rat CCK1R (rCCK1R-Ala<sup>317,321,325</sup>) that had previously been fully characterized as interfering with oligomerization (non-dimerizing) and demonstrated to exhibit normal CCK binding and biological responses<sup>14</sup> was also utilized in a specific series of studies, following transient expression in COS cells.

### Receptor-enriched cell membranes

Receptor-bearing membrane fractions enriched in plasma membranes were isolated from the cell lines, as described previously<sup>40</sup>. In brief, cells were harvested in ice-cold phosphate-buffered saline, pH 7.4. The membrane fraction of interest was separated and isolated using sucrose-density gradient centrifugation, and was suspended in Krebs-Ringer-HEPES (KRH) medium (25 mM HEPES, pH 7.4, 104 mM NaCl, 5 mM KCl, 1.5 mM CaCl<sub>2</sub>, 1.0 mM KH<sub>2</sub>PO<sub>4</sub>, 1.2 mM MgSO<sub>4</sub>, 1.2 mM MgCl<sub>2</sub>) containing 0.01% soybean trypsin inhibitor and 1 mM phenylmethylsulfonyl fluoride. Membranes were stored at -80°C until use.

### Receptor binding assays

Receptor ligand competition-binding assays were performed as described previously<sup>11</sup>, using CCK-like or benzodiazepine radioligands. Assay conditions that have previously been described and utilized<sup>5, 12, 41</sup> were carried out in duplicate by incubating membrane suspensions (4–7 µg of protein/sample) in the absence or presence of increasing concentrations of unlabeled CE-326597 or PF-04756956 and radioligand (~20–25 pM) in KRH medium at room temperature for 60 min. Saturable binding was determined in each case using unlabeled CCK or the same benzodiazepine as utilized in the radioligand binding assay, with IC<sub>50</sub> values determined based on inhibition of 50 percent of this saturable binding. Control experiments, including incubations as long as 24 h, were performed to be certain that binding had achieved equilibrium conditions. Receptor-bound and free radioligand were separated by vacuum filtration using Unifilter-96 well microplates with

bonded GF/B filters in a Filtermate Harvester (PerkinElmer, Waltham, MA). The plates were washed six times with wash buffer (0.9% NaCl and 0.2% bovine serum albumin), air-dried, soaked in 30  $\mu$ l of Microscint<sup>TM</sup>, and radioactivity was quantified using a Top CountNXT<sup>TM</sup> instrument (Packard, Meriden, CT). Non-saturable binding was determined by measuring the amount of radioactivity bound in the presence of 1  $\mu$ M unlabeled BDZ ligands or 1  $\mu$ M CCK in the respective assays.

### Intracellular calcium assays

Biological activity of CE-326597 or PF-04756956 at the various CCK receptor-based mutants was measured by quantifying intracellular calcium responses in intact cells<sup>42–44</sup>. These responses are reported as percentages of maximal responses to 10 nM CCK. In brief, approximately 24 h before the assay, cells were seeded in sterile clear-bottom black 96-well tissue culture plates so that they reached approximate confluence of 70–80% at the time of the assay. Cells were incubated with 1.5  $\mu$ M Quest Fluo 8AM (dissolved in anhydrous DMSO) for 1 h at 37°C in the dark, after washing once with KRH medium containing 2.5 mM probenecid and 0.2% bovine serum albumin. After the incubation, the cells were washed once with KRH medium, and the assay was performed in a Flexstation 3.0 plate reader (Molecular Devices, Sunnyvale, CA) using robotic addition of the appropriate agonist ligand. Intracellular calcium responses were measured at 37°C by measuring the fluorescence emission intensity at 525 nm after excitation at 485 nm, with data collection every 4 sec over a 120 sec period. Data were plotted, providing the identification of peak responses and EC<sub>50</sub> concentrations.

### Molecular Modeling

All molecular modeling was conducted using a stochastic global energy optimization procedure in Internal Coordinate Mechanics (ICM)<sup>45</sup> with the ICM-Pro package version 3.8–4 (MolSoft LLC, San Diego, CA) This procedure consisted of three iterative steps: (a) random conformational change of groups of dihedral angles and positional variables according to the biased-probability Monte Carlo method<sup>46</sup>; (b) local minimization of all free dihedral angles; and (c) acceptance or rejection of the new conformation based on the Metropolis criterion at the simulation temperature, usually at 600 K<sup>47</sup>.

The ligand-guided homology modeling method<sup>48</sup> that we previously used to construct the active form of the type 1 CCK receptor model<sup>5</sup> was utilized in this work. The previously-built model of the active form of this receptor was used as the starting point for the current modeling. A collection of 159 type 1 CCK receptor agonist ligands selected from the ChEMBL database<sup>49</sup> was used to refine the ligand binding pocket of the active structure. PF-04756956 was first docked to the active form. A distance restraint was used between the ligand and an anchor residue on the receptor to limit the size of the sampling space and to keep the ligand within the pocket during the molecular modeling process. Previously, after attempting to use several different hydrogen bond donor-acceptor pairs, the best models were found to come from use of Asn 6.55 as the anchor residue<sup>11</sup>. A defined hydrogen bond distance restraint with this residue was used during the simulations, and each ligand was docked to the pocket followed by cycles of stochastic global energy optimization, side chain sampling, backbone minimization, and loop modeling. This resulted in an ensemble of

multiple receptor conformations for the PF-04756956-bound type 1 CCK receptor active structure.

Each pocket conformation in the ensemble was then evaluated using a composite score that included the ability to differentiate structurally diverse positives from decoys by docking scores, the percentage of ligands forming hydrogen bonds with the anchor residue (Asn 6.55), and the consistency of ligand binding poses based on clustering of these poses as assessed by Atomic Property Fields<sup>50</sup>. The best model was then assessed using plots of receiver operating characteristic (ROC) curves<sup>51</sup> to evaluate the ability to differentiate the set of 159 known type 1 CCK receptor agonists having activities greater than 1  $\mu$ M seeded into 1739 non-agonist ligands of the type 1 CCK receptor ligands present in the ChEMBL database.

### Data Analysis and Statistics

All data were analyzed using Prism 5 (GraphPad Software, Inc., San Diego, CA). In all analyses, the data were unweighted, with the mean of replicates in each experiment considered as an individual point. Concentration-response data were analyzed using the three-parameter logistic equation described by May et al.<sup>52</sup>:  $E = \text{Bottom} + ((\text{Top} - \text{Bottom}) [A]) / ([A] + [EC_{50}])$ , where Bottom represents the E value in the absence of ligand, Top represents the maximal stimulation in the presence of ligand, [A] is the molar concentration of ligand, and  $EC_{50}$  represents the molar concentration of ligand required to generate a response halfway between Top and Bottom. The same equation was used for competition binding data, with  $IC_{50}$  replacing  $EC_{50}$ .  $IC_{50}$  values were corrected for radioligand occupancy using the Cheng Prusoff equation<sup>53</sup>. Competitive and allosteric ternary complex models<sup>13</sup> were utilized for the analysis of the binding data. Differences in receptor binding and signaling parameters between various constructs were statistically evaluated using unpaired t-tests, with  $p < 0.05$  considered to be significant.

### Acknowledgments

This work was supported by grants from the National Institutes of Health (DK032878 to L.J.M. and GM071872 to R.A.) and by the Mayo Clinic. A.C. and P.M.S. are Principal Research Fellows of the National Health and Medical Research Council of Australia. The authors would like to thank Dr. Kimberly O. Cameron at Pfizer Global Research and Development in Groton, CT for providing insights into structure-activity considerations related to this work and for providing the key compounds for this effort through the Pfizer Compound Transfer Program. The authors would like to acknowledge Professor P.S. Portoghese of the University of Minnesota for kindly providing BDZ-1 and BDZ-2 compounds. The authors would also like to acknowledge the excellent technical assistance of M.L. Augustine and A.M. Ball.

### ABBREVIATIONS USED

<b>BDZ</b>	benzodiazepine
<b>CCK</b>	cholecystokinin
<b>CCK1R</b>	type 1 cholecystokinin receptor
<b>CCK2R</b>	type 2 cholecystokinin receptor
<b>TM</b>	transmembrane

<b>CHO</b>	Chinese hamster ovary
<b>GPCR</b>	G protein-coupled receptor
<b>KRH</b>	Krebs-Ringer's-HEPES

## References

1. Kissileff HR, Pi-Sunyer FX, Thornton J, Smith GP. C-terminal octapeptide of cholecystokinin decreases food intake in man. *Am J Clin Nutr.* 1981; 34:154–60. [PubMed: 6259918]
2. Li Y, Owyang C. Endogenous cholecystokinin stimulates pancreatic enzyme secretion via vagal afferent pathway in rats. *Gastroenterology.* 1994; 107:525–31. [PubMed: 8039628]
3. Dockray GJ. Cholecystokinin and gut-brain signalling. *Regul Pept.* 2009; 155:6–10. [PubMed: 19345244]
4. Smith GP, Gibbs J. The satiety effect of cholecystokinin. Recent progress and current problems. *Ann N Y Acad Sci.* 1985; 448:417–23. [PubMed: 3896096]
5. Harikumar KG, Cawston EE, Lam PC, Patil A, Orry A, Henke BR, Abagyan R, Christopoulos A, Sexton PM, Miller LJ. Molecular basis for benzodiazepine agonist action at the type 1 cholecystokinin receptor. *J Biol Chem.* 2013; 288:21082–95. [PubMed: 23754289]
6. Aquino CJ, Armour DR, Berman JM, Birkemo LS, Carr RA, Croom DK, Dezube M, Dougherty RW Jr, Ervin GN, Grizzle MK, Head JE, Hirst GC, James MK, Johnson MF, Miller LJ, Queen KL, Rimele TJ, Smith DN, Sugg EE. Discovery of 1,5-benzodiazepines with peripheral cholecystokinin (CCK-A) receptor agonist activity. 1. Optimization of the agonist “trigger”. *J Med Chem.* 1996; 39:562–9. [PubMed: 8558528]
7. Ballesteros JA, Weinstein H. Analysis and refinement of criteria for predicting the structure and relative orientations of transmembranal helical domains. *Biophys J.* 1992; 62:107–9. [PubMed: 1600090]
8. Elliott RL, Cameron KO, Chin JE, Bartlett JA, Beretta EE, Chen Y, da Jardine PS, Dubins JS, Gillaspay ML, Hargrove DM, Kalgutkar AS, LaFlamme JA, Lame ME, Martin KA, Maurer TS, Nardone NA, Oliver RM, Scott DO, Sun D, Swick AG, Trebino CE, Zhang Y. Discovery of N-benzyl-2-[(4S)-4-(1H-indol-3-ylmethyl)-5-oxo-1-phenyl-4,5-dihydro-6H-[1,2,4]triazolo[4,3-a][1,5]benzodiazepin-6-yl]-N-isopropylacetamide, an orally active, gut-selective CCK1 receptor agonist for the potential treatment of obesity. *Bioorg Med Chem Lett.* 2010; 20:6797–801. [PubMed: 20851601]
9. Cameron KO, Beretta EE, Chen Y, Chu-Moyer M, Fernando D, Gao H, Kohrt J, Lavergne S, da Jardine PS, Guzman-Perez A, Hoth C, Perry DA, Hadcock JR, Gautreau D, Makowski M, Perez S, Polivkova J, Rogers L, Scott DO, Swick AG, Thiede L, Trebino CE, Trilles RV, Wilmowski J, Zhang Y. Discovery of new piperidine amide triazolobenzodiazepinones as intestinal-selective CCK1 receptor agonists. *Bioorg Med Chem Lett.* 2012; 22:2943–7. [PubMed: 22424974]
10. Akgun E, Korner M, Gao F, Harikumar KG, Waser B, Reubi JC, Portoghese PS, Miller LJ. Synthesis and in vitro characterization of radioiodinatable benzodiazepines selective for type 1 and type 2 cholecystokinin receptors. *J Med Chem.* 2009; 52:2138–47. [PubMed: 19271701]
11. Cawston EE, Lam PC, Harikumar KG, Dong M, Ball AM, Augustine ML, Akgun E, Portoghese PS, Orry A, Abagyan R, Sexton PM, Miller LJ. Molecular basis for binding and subtype selectivity of 1,4-benzodiazepine antagonist ligands of the cholecystokinin receptor. *J Biol Chem.* 2012; 287:18618–35. [PubMed: 22467877]
12. Gao F, Sexton PM, Christopoulos A, Miller LJ. Benzodiazepine ligands can act as allosteric modulators of the Type 1 cholecystokinin receptor. *Bioorg Med Chem Lett.* 2008; 18:4401–4. [PubMed: 18621527]
13. Christopoulos A, Kenakin T. G protein-coupled receptor allostery and complexing. *Pharmacol Rev.* 2002; 54:323–74. [PubMed: 12037145]

14. Harikumar KG, Dong M, Cheng Z, Pinon DI, Lybrand TP, Miller LJ. Transmembrane segment peptides can disrupt cholecystokinin receptor oligomerization without affecting receptor function. *Biochemistry*. 2006; 45:14706–16. [PubMed: 17144663]
15. Chaudhri OB, Salem V, Murphy KG, Bloom SR. Gastrointestinal satiety signals. *Annu Rev Physiol*. 2008; 70:239–55. [PubMed: 17937600]
16. Gibbs J, Young RC, Smith GP. Cholecystokinin decreases food intake in rats. *J Comp Physiol Psychol*. 1973; 84:488–95. [PubMed: 4745816]
17. Asin KE, Bednarz L, Nikkel AL, Gore PA Jr, Montana WE, Cullen MJ, Shiosaki K, Craig R, Nadzan AM. Behavioral effects of A71623; a highly selective CCK-A agonist tetrapeptide. *Am J Physiol*. 1992; 263:R125–35. [PubMed: 1636779]
18. Castillo EJ, Delgado-Aros S, Camilleri M, Burton D, Stephens D, O'Connor-Semmes R, Walker A, Shachoy-Clark A, Zinsmeister AR. Effect of oral CCK-1 agonist GI181771X on fasting and postprandial gastric functions in healthy volunteers. *Am J Physiol Gastrointest Liver Physiol*. 2004; 287:G363–9. [PubMed: 15246968]
19. Berger R, Zhu C, Hansen AR, Harper B, Chen Z, Holt TG, Hubert J, Lee SJ, Pan J, Qian S, Reitman ML, Strack AM, Weingarh DT, Wolff M, Macneil DJ, Weber AE, Edmondson SD. 2-Substituted piperazine-derived imidazole carboxamides as potent and selective CCK1R agonists for the treatment of obesity. *Bioorg Med Chem Lett*. 2008; 18:4833–7. [PubMed: 18684621]
20. Bignon E, Alonso R, Arnone M, Boigegrain R, Brodin R, Gueudet C, Heaulme M, Keane P, Landi M, Molimard JC, Olliero D, Poncelet M, Seban E, Simiand J, Soubrie P, Pascal M, Maffrand JP, Le Fur G. SR146131: a new potent, orally active, and selective nonpeptide cholecystokinin subtype 1 receptor agonist. II. In vivo pharmacological characterization. *J Pharmacol Exp Ther*. 1999; 289:752–61. [PubMed: 10215649]
21. Smith JP, Solomon TE. Cholecystokinin and pancreatic cancer: the chicken or the egg? *Am J Physiol Gastrointest Liver Physiol*. 2014; 306:G91–G101. [PubMed: 24177032]
22. Dawra R, Saluja A, Lerch MM, Saluja M, Logsdon C, Steer M. Stimulation of pancreatic growth by cholecystokinin is mediated by high affinity receptors on rat pancreatic acinar cells. *Biochem Biophys Res Commun*. 1993; 193:814–20. [PubMed: 8323557]
23. Katritch V, Cherezov V, Stevens RC. Structure-function of the G protein-coupled receptor superfamily. *Annu Rev Pharmacol Toxicol*. 2013; 53:531–56. [PubMed: 23140243]
24. Venkatakrishnan AJ, Deupi X, Lebon G, Tate CG, Schertler GF, Babu MM. Molecular signatures of G-protein-coupled receptors. *Nature*. 2013; 494:185–94. [PubMed: 23407534]
25. Beinborn M, Lee YM, McBride EW, Quinn SM, Kopin AS. A single amino acid of the cholecystokinin-B/gastrin receptor determines specificity for non-peptide antagonists. *Nature*. 1993; 362:348–50. [PubMed: 8455720]
26. Gouldson P, Legoux P, Carillon C, Delpech B, Le Fur G, Ferrara P, Shire D. The agonist SR 146131 and the antagonist SR 27897 occupy different sites on the human CCK(1) receptor. *Eur J Pharmacol*. 2000; 400:185–94. [PubMed: 10988332]
27. Escricuet C, Gigoux V, Archer E, Verrier S, Maigret B, Behrendt R, Moroder L, Bignon E, Silvente-Poirot S, Pradayrol L, Fourmy D. The biologically crucial C terminus of cholecystokinin and the non-peptide agonist SR-146,131 share a common binding site in the human CCK1 receptor. Evidence for a crucial role of Met-121 in the activation process. *J Biol Chem*. 2002; 277:7546–55. [PubMed: 11724786]
28. Hadac EM, Dawson ES, Darrow JW, Sugg EE, Lybrand TP, Miller LJ. Novel benzodiazepine photoaffinity probe stereoselectively labels a site deep within the membrane-spanning domain of the cholecystokinin receptor. *J Med Chem*. 2006; 49:850–63. [PubMed: 16451051]
29. Ji Z, Hadac EM, Henne RM, Patel SA, Lybrand TP, Miller LJ. Direct identification of a distinct site of interaction between the carboxyl-terminal residue of cholecystokinin and the type A cholecystokinin receptor using photoaffinity labeling. *J Biol Chem*. 1997; 272:24393–401. [PubMed: 9305898]
30. Ding XQ, Dolu V, Hadac EM, Holicky EL, Pinon DI, Lybrand TP, Miller LJ. Refinement of the structure of the ligand-occupied cholecystokinin receptor using a photolabile amino-terminal probe. *J Biol Chem*. 2001; 276:4236–44. [PubMed: 11050076]



31. Martin-Martinez M, Marty A, Jourdan M, Escrieux C, Archer E, Gonzalez-Muniz R, Garcia-Lopez MT, Maigret B, Herranz R, Fourmy D. Combination of molecular modeling, site-directed mutagenesis, and SAR studies to delineate the binding site of pyridopyrimidine antagonists on the human CCK1 receptor. *J Med Chem*. 2005; 48:4842–50. [PubMed: 16033264]
32. Hadac EM, Pinon DI, Ji Z, Holicky EL, Henne RM, Lybrand TP, Miller LJ. Direct identification of a second distinct site of contact between cholecystokinin and its receptor. *J Biol Chem*. 1998; 273:12988–93. [PubMed: 9582333]
33. Arlander SJ, Dong M, Ding XQ, Pinon DI, Miller LJ. Key differences in molecular complexes of the cholecystokinin receptor with structurally related peptide agonist, partial agonist, and antagonist. *Mol Pharmacol*. 2004; 66:545–52. [PubMed: 15322246]
34. Dong M, Liu G, Pinon DI, Miller LJ. Differential docking of high-affinity peptide ligands to type A and B cholecystokinin receptors demonstrated by photoaffinity labeling. *Biochemistry*. 2005; 44:6693–700. [PubMed: 15850403]
35. Dong M, Lam PC, Pinon DI, Abagyan R, Miller LJ. Elucidation of the molecular basis of cholecystokinin Peptide docking to its receptor using site-specific intrinsic photoaffinity labeling and molecular modeling. *Biochemistry*. 2009; 48:5303–12. [PubMed: 19441839]
36. Harikumar KG, Pinon DI, Miller LJ. Fluorescent indicators distributed throughout the pharmacophore of cholecystokinin provide insights into distinct modes of binding and activation of type A and B cholecystokinin receptors. *J Biol Chem*. 2006; 281:27072–80. [PubMed: 16857665]
37. Harikumar KG, Gao F, Pinon DI, Miller LJ. Use of multidimensional fluorescence resonance energy transfer to establish the orientation of cholecystokinin docked at the type A cholecystokinin receptor. *Biochemistry*. 2008; 47:9574–81. [PubMed: 18700727]
38. Dong M, Vattelana AM, Lam PC, Orry AJ, Abagyan R, Christopoulos A, Sexton PM, Haines DR, Miller LJ. Development of a highly selective allosteric antagonist radioligand for the type 1 cholecystokinin receptor and elucidation of its molecular basis of binding. *Mol Pharmacol*. 2015; 87:130–40. [PubMed: 25319540]
39. Pearson RK, Miller LJ, Powers SP, Hadac EM. Biochemical characterization of the pancreatic cholecystokinin receptor using monofunctional photoactivatable probes. *Pancreas*. 1987; 2:79–84. [PubMed: 3575316]
40. Hadac EM, Ghanekar DV, Holicky EL, Pinon DI, Dougherty RW, Miller LJ. Relationship between native and recombinant cholecystokinin receptors: role of differential glycosylation. *Pancreas*. 1996; 13:130–9. [PubMed: 8829180]
41. Desai AJ, Henke BR, Miller LJ. Elimination of a cholecystokinin receptor agonist ‘trigger’ in an effort to develop positive allosteric modulators without intrinsic agonist activity. *Bioorg Med Chem Lett*. 2015; 25:1849–55. [PubMed: 25862198]
42. Harikumar KG, Potter RM, Patil A, Echeveste V, Miller LJ. Membrane cholesterol affects stimulus-activity coupling in type 1, but not type 2, CCK receptors: use of cell lines with elevated cholesterol. *Lipids*. 2013; 48:231–44. [PubMed: 23306829]
43. Desai AJ, Harikumar KG, Miller LJ. A type 1 cholecystokinin receptor mutant that mimics the dysfunction observed for wild type receptor in a high cholesterol environment. *J Biol Chem*. 2014; 289:18314–26. [PubMed: 24825903]
44. Desai AJ, Dong M, Harikumar KG, Miller LJ. Impact of ursodeoxycholic acid on a CCK1R cholesterol-binding site may contribute to its positive effects in digestive function. *Am J Physiol Gastrointest Liver Physiol*. 2015; 309:G377–86. [PubMed: 26138469]
45. Abagyan R, Totrov M, Kuznetsov D. ICM—A new method for protein modeling and design: Applications to docking and structure prediction from the distorted native conformation. *Journal of Computational Chemistry*. 1994; 15:488–506.
46. Abagyan R, Totrov M. Biased probability Monte Carlo conformational searches and electrostatic calculations for peptides and proteins. *J Mol Biol*. 1994; 235:983–1002. [PubMed: 8289329]
47. Metropolis N, Rosenbluth AW, Rosenbluth MN, Teller AH, Teller E. Equation of State Calculations by Fast Computing Machines. *The Journal of Chemical Physics*. 1953; 21:1087–1092.

48. Katritch V, Rueda M, Lam PC, Yeager M, Abagyan R. GPCR 3D homology models for ligand screening: lessons learned from blind predictions of adenosine A2a receptor complex. *Proteins*. 2010; 78:197–211. [PubMed: 20063437]
49. Overington J. ChEMBL. An interview with John Overington, team leader, chemogenomics at the European Bioinformatics Institute Outstation of the European Molecular Biology Laboratory (EMBL-EBI). Interview by Wendy A. Warr. *J Comput Aided Mol Des*. 2009; 23:195–8. [PubMed: 19194660]
50. Totrov M. Atomic property fields: generalized 3D pharmacophoric potential for automated ligand superposition, pharmacophore elucidation and 3D QSAR. *Chem Biol Drug Des*. 2008; 71:15–27. [PubMed: 18069986]
51. Truchon JF, Bayly CI. Evaluating virtual screening methods: good and bad metrics for the “early recognition” problem. *J Chem Inf Model*. 2007; 47:488–508. [PubMed: 17288412]
52. May LT, Avlani VA, Langmead CJ, Herdon HJ, Wood MD, Sexton PM, Christopoulos A. Structure-function studies of allosteric agonism at M2 muscarinic acetylcholine receptors. *Mol Pharmacol*. 2007; 72:463–76. [PubMed: 17525129]
53. Cheng Y, Prusoff WH. Relationship between the inhibition constant (K<sub>1</sub>) and the concentration of inhibitor which causes 50 per cent inhibition (I<sub>50</sub>) of an enzymatic reaction. *Biochem Pharmacol*. 1973; 22:3099–108. [PubMed: 4202581]

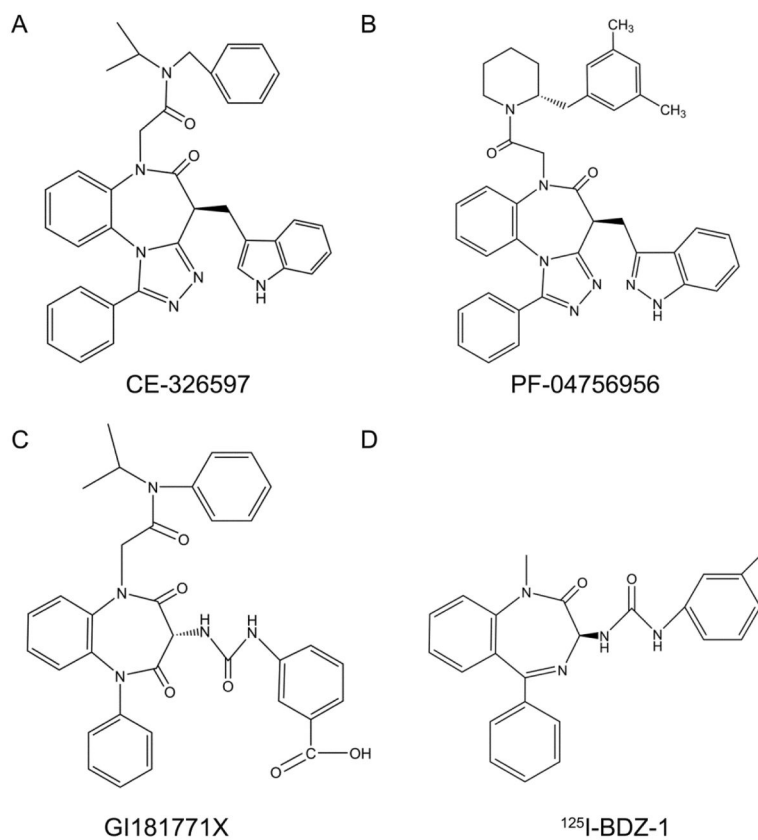


**Figure 1. Structures of key CCK1R ligands**

Shown are the chemical structures of CE-326597 (A) and PF-04756956 (B), as well as GI181771X (C) and the BDZ-1 allosteric antagonist radioligand (D) used in this work.

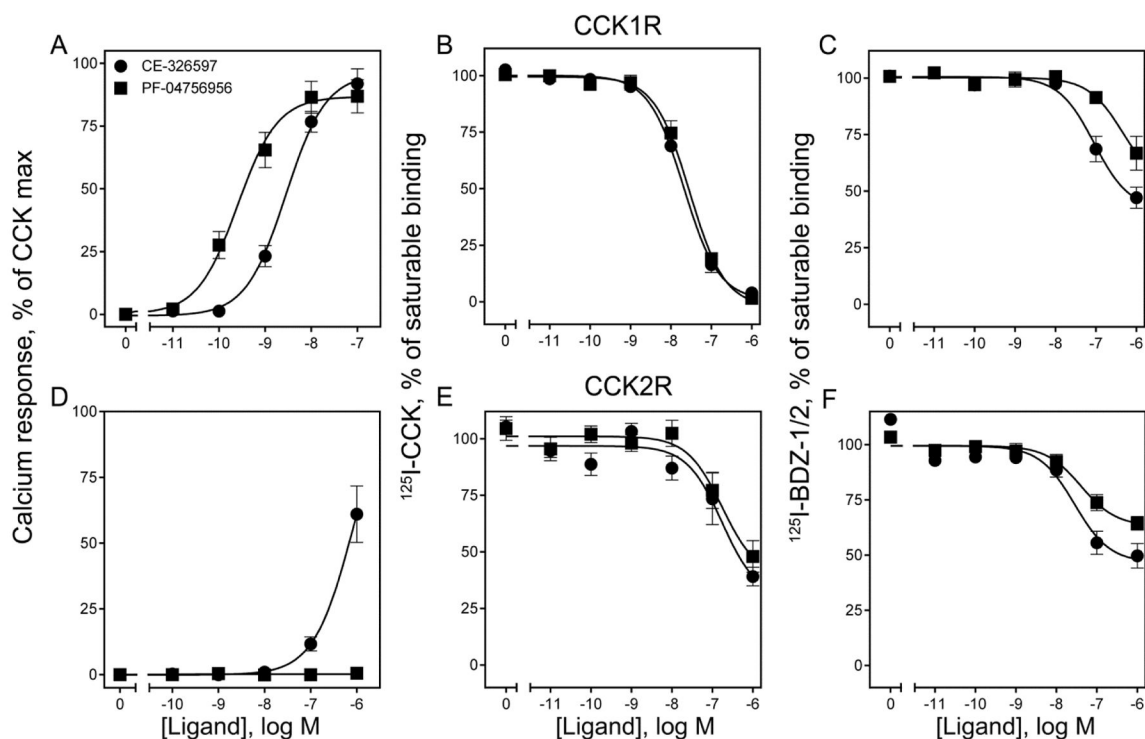


**Figure 2. Biological activity and binding of CE-326597 and PF-04756956 at wild type CCK1R and CCK2R**

Shown are the intracellular calcium responses of these compounds at both subtypes of CCK receptors expressed on CHO-CCK1R (top row) and CHO-CCK2R (bottom row) cells (A, D). Also shown are the data from competition-binding experiments with the orthosteric radioligand,  $^{125}\text{I}$ -CCK (B, E), or the allosteric radioligands,  $^{125}\text{I}$ -BDZ-1 or 2 (C, F) at the CCK1R or the CCK2R expressed on CHO membranes respectively. The X-axis values reflect the absence of ligand (0) to the left of the break, and log molar concentrations to the right of the break. Biological activity data are represented as percentages of the maximal responses of each cell line to 10 nM concentration of natural agonist, CCK. Non-saturable binding was determined by using 1  $\mu\text{M}$  unlabeled BDZ or CCK. Data are represented as means  $\pm$  S.E.M. from duplicate determinations from at least five independent experiments.

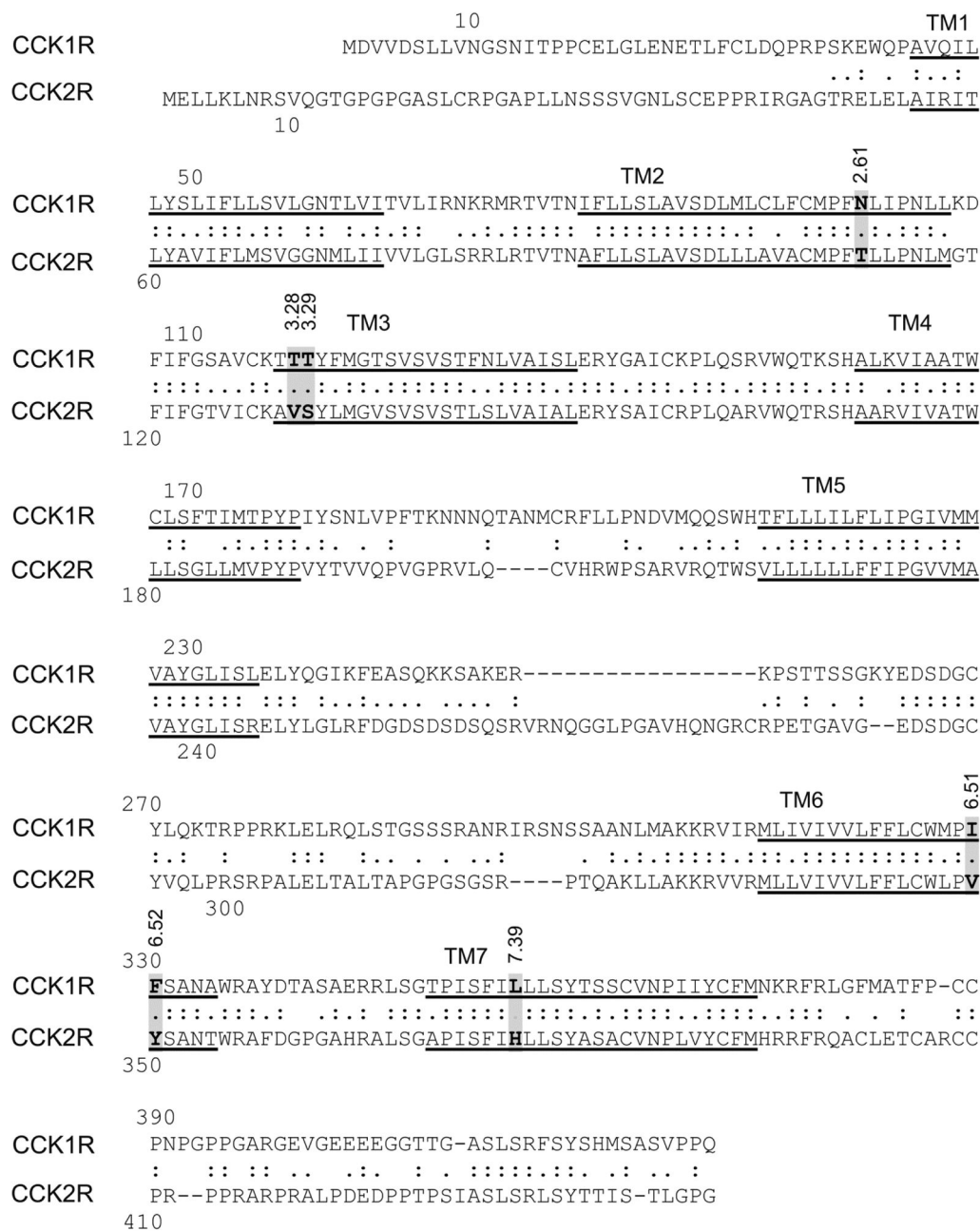


**Figure 3. Primary sequence alignment of human CCK1R and CCK2R**  
 Shown is an alignment of the sequences of the human CCK1R and CCK2R, identifying predicted transmembrane (TM) segments (underlined), as well as the residues believed to line the intramembranous pocket that are distinct in these two receptors. These residues were exchanged in the chimeric constructs utilized for this project.

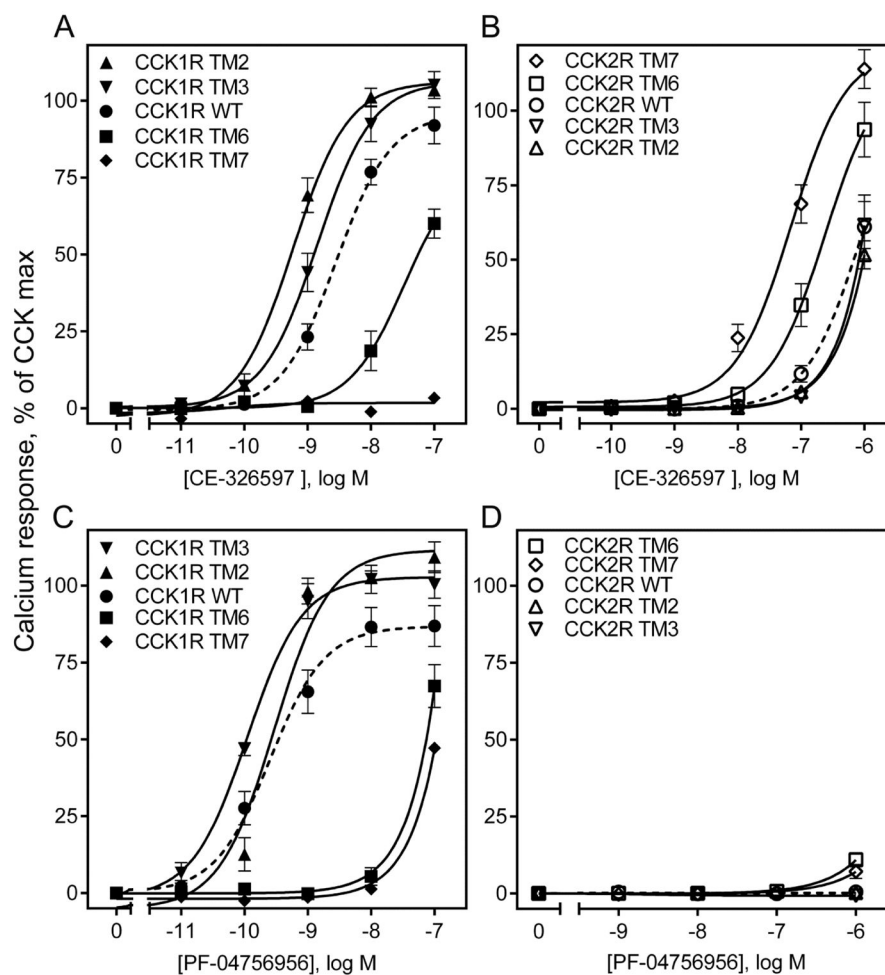


**Figure 4. Biological activity at CCK1R- and CCK2R-based chimeric receptor constructs**  
 The curves shown here are representative of the abilities of CE-326597 (top row) and PF-04756956 (bottom row) to stimulate intracellular calcium responses in the CCK1R (A, C) or CCK2R (B, D) wild type and chimeric constructs bearing CHO cells. The X-axis values reflect the absence of ligand (0) to the left of the break, and log molar concentrations to the right of the break. Data are represented as percentages of the maximal responses of each cell line to 10 nM concentration of natural agonist, CCK. Data are expressed as means  $\pm$  S.E.M. of duplicate determinations from at least three to nine independent experiments.

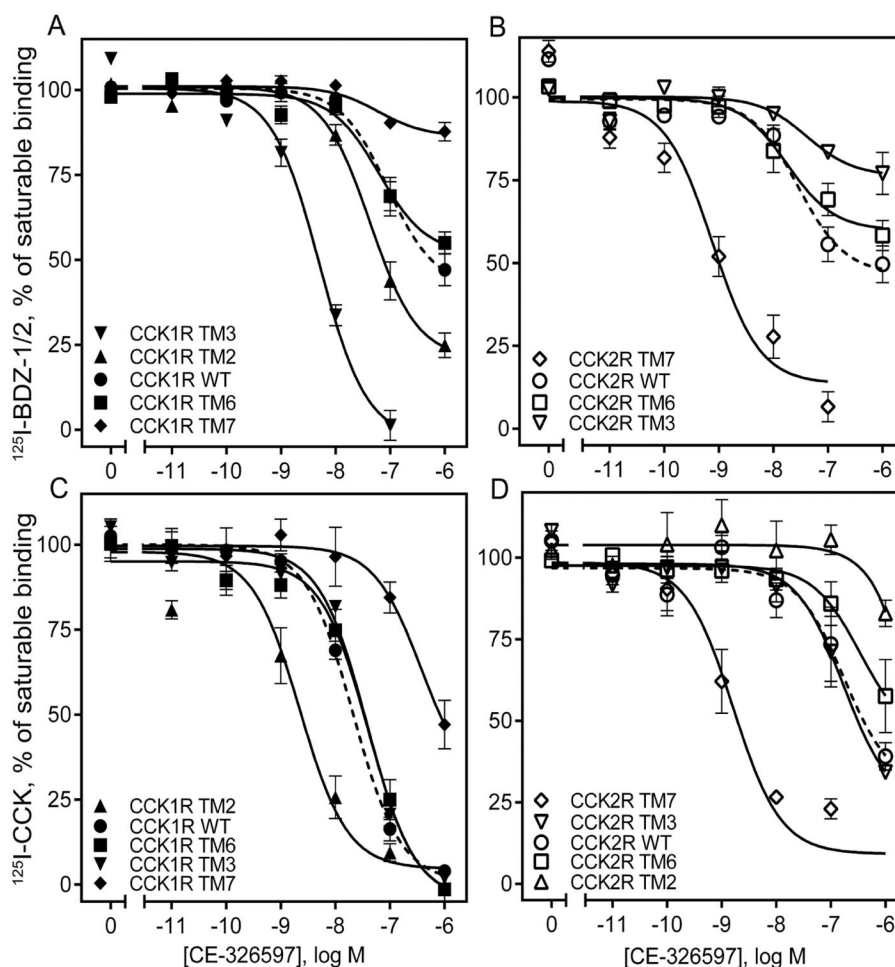


**Figure 5. Competition-binding studies of CE-326597 using CCK1R- and CCK2R-based chimeric receptor constructs**

Shown are the competition-binding curves for CE-326597 at CCK1R (A, C) or CCK2R (B, D) based TM chimeric constructs using the allosteric antagonist radiolabels,  $^{125}\text{I}$ -BDZ-1 (for CCK1R) (A),  $^{125}\text{I}$ -BDZ-2 (for CCK2R) (B), or orthosteric CCK-like radiolabel (C, D). The X-axis values reflect the absence of ligand (0) to the left of the break, and log molar concentrations to the right of the break. Values represent percentages of maximal saturable binding that were observed in the absence of competitor. Non-saturable binding was determined by using 1  $\mu\text{M}$  unlabeled BDZ-1 or BDZ-2, as appropriate for the radioligand, or CCK. Data are expressed as means  $\pm$  S.E.M. of duplicate determinations from four to six independent experiments.

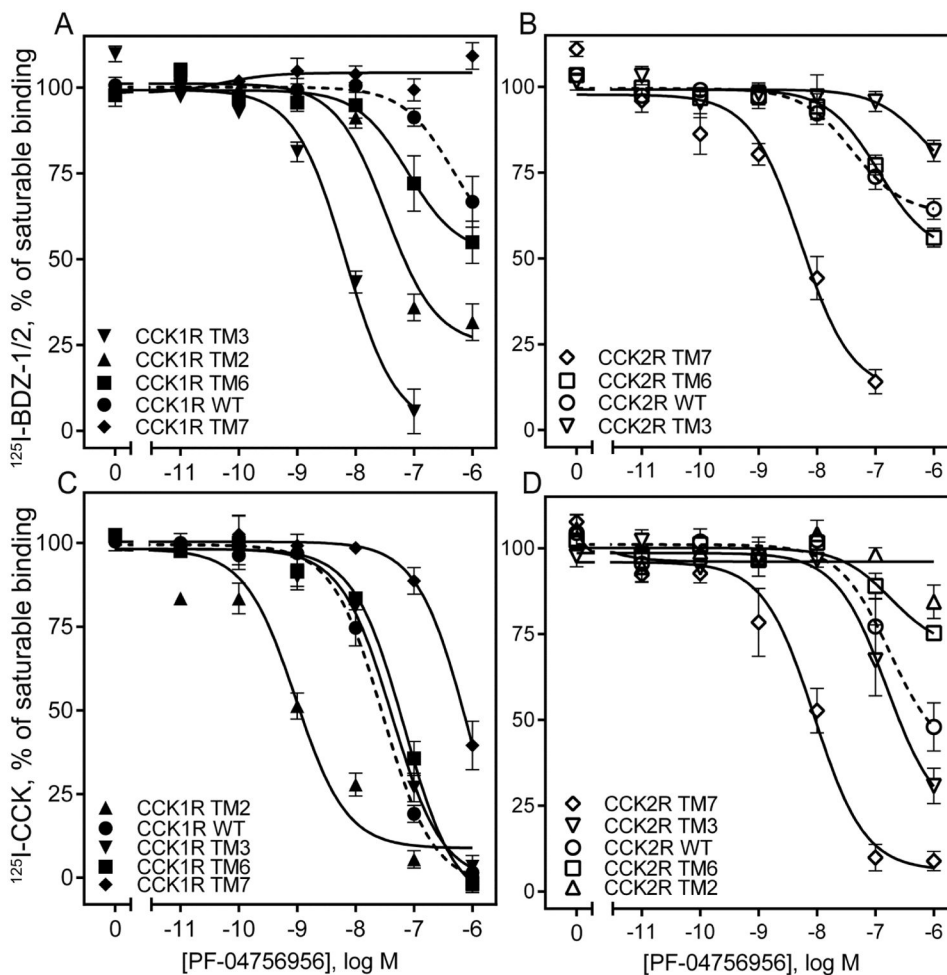


**Figure 6. Competition-binding studies of PF-04756956 using CCK1R- and CCK2R-based chimeric receptor constructs**

Shown are the competition-binding curves for PF-04756956 at CCK1R (A, C) or CCK2R (B, D) based TM chimeric constructs using the allosteric antagonist radiolabels,  $^{125}\text{I}$ -BDZ-1 (for CCK1R) (A),  $^{125}\text{I}$ -BDZ-2 (for CCK2R) (B), or orthosteric CCK-like radiolabel (C, D). The X-axis values reflect the absence of ligand (0) to the left of the break, and log molar concentrations to the right of the break. Values represent percentages of maximal saturable binding that were observed in the absence of competitor. Non-saturable binding was determined by using 1  $\mu\text{M}$  unlabeled BDZ-1 or BDZ-2, as appropriate for the radioligand, or CCK. Data are expressed as means  $\pm$  S.E.M. of duplicate determinations from four to six independent experiments.



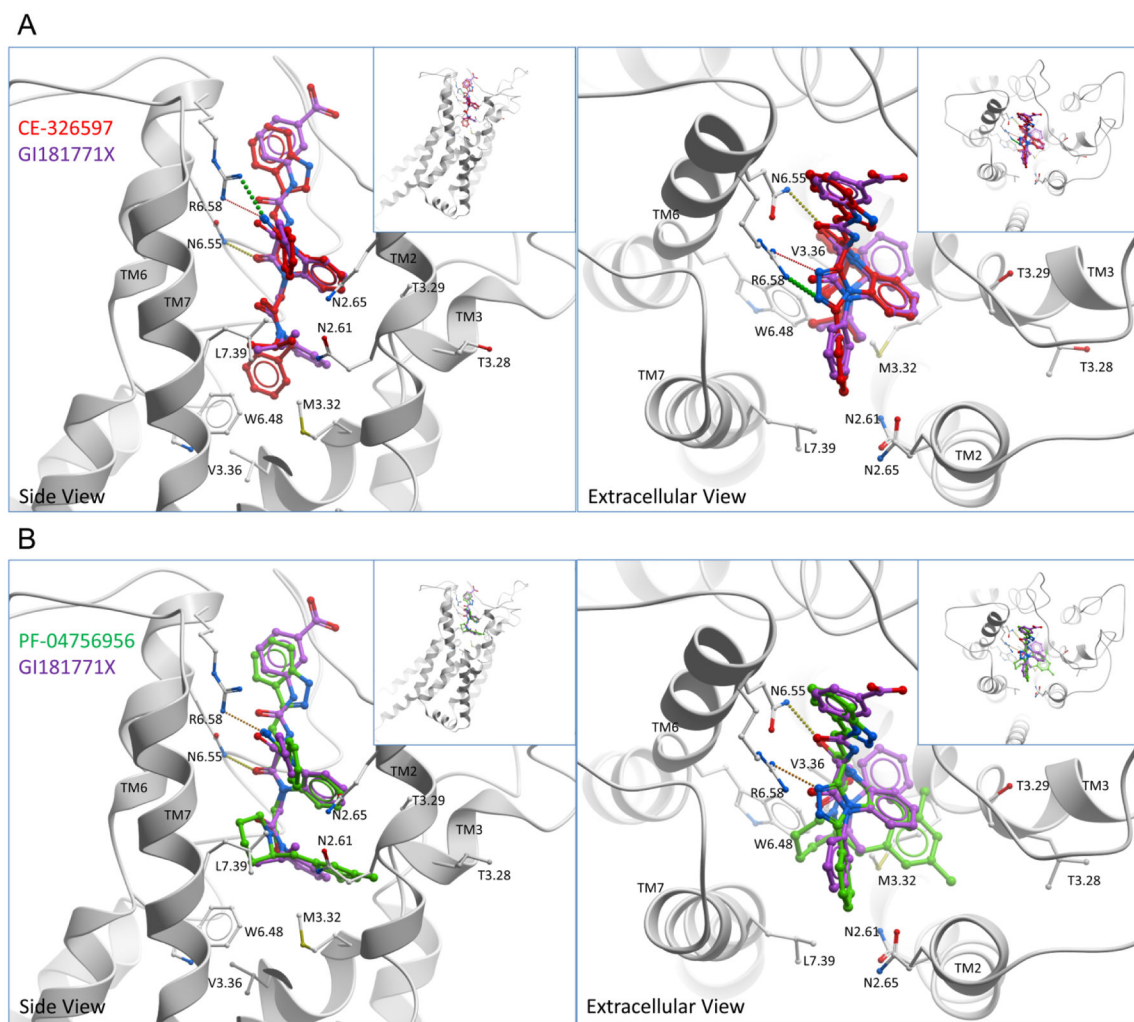


**Figure 7. Comparison of docked binding poses of CE-326597 and PF-04756956 at CCK1R with that of GI181771X**

Shown are the best performing model for docked binding poses of CE-326597 (red stick) (A), and PF-04756956 (green stick) (B) compared to the previously described docking pose of GI181771X (purple stick). The viewpoint in the left panels is from the side within the membrane, whereas the viewpoint in the right panels is from above the membrane. Hydrogen bonds are represented as small colored spheres. TM1 has been cut away in the side view.

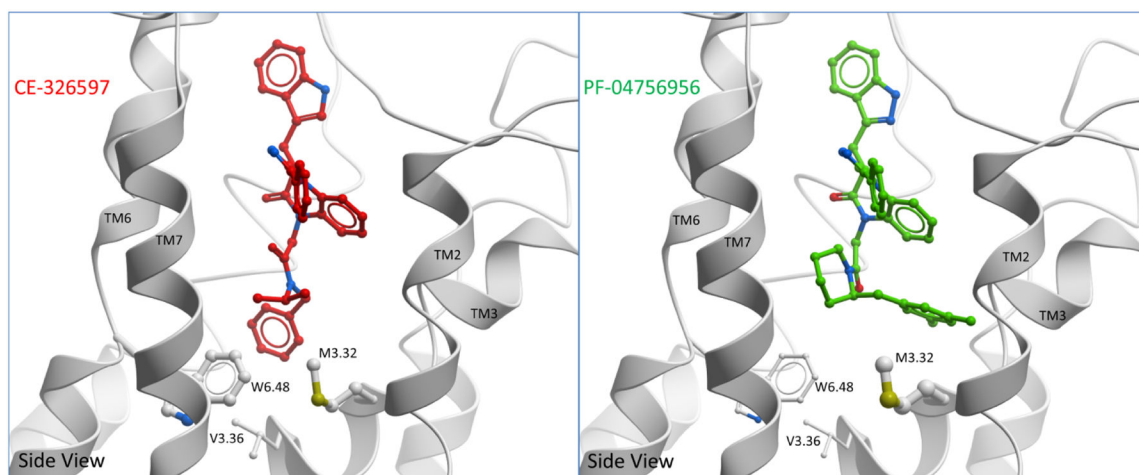


**Figure 8. Comparison of docked binding poses of CE-326597 and PF-04756956 at CCK1R**  
Shown are the best performing models illustrating the docking pose of CE-326597 (left) and PF-04756956 (right) from a side view. The binding poses of both compounds were predicted to be accommodated in a similar pocket, however the differences between the two are marked by the position of the N1-benzyl (CE-326597) that is buried deeper, and the dimethyl benzyl at C2 position of piperidine (PF-04756956) that is more superficially located. Also shown are potential interacting residues, Trp 6.48, Met 3.32 and Val 3.36. Large contact areas between the side-chain and ligand are represented by thicker stick representation on the mutated residues.

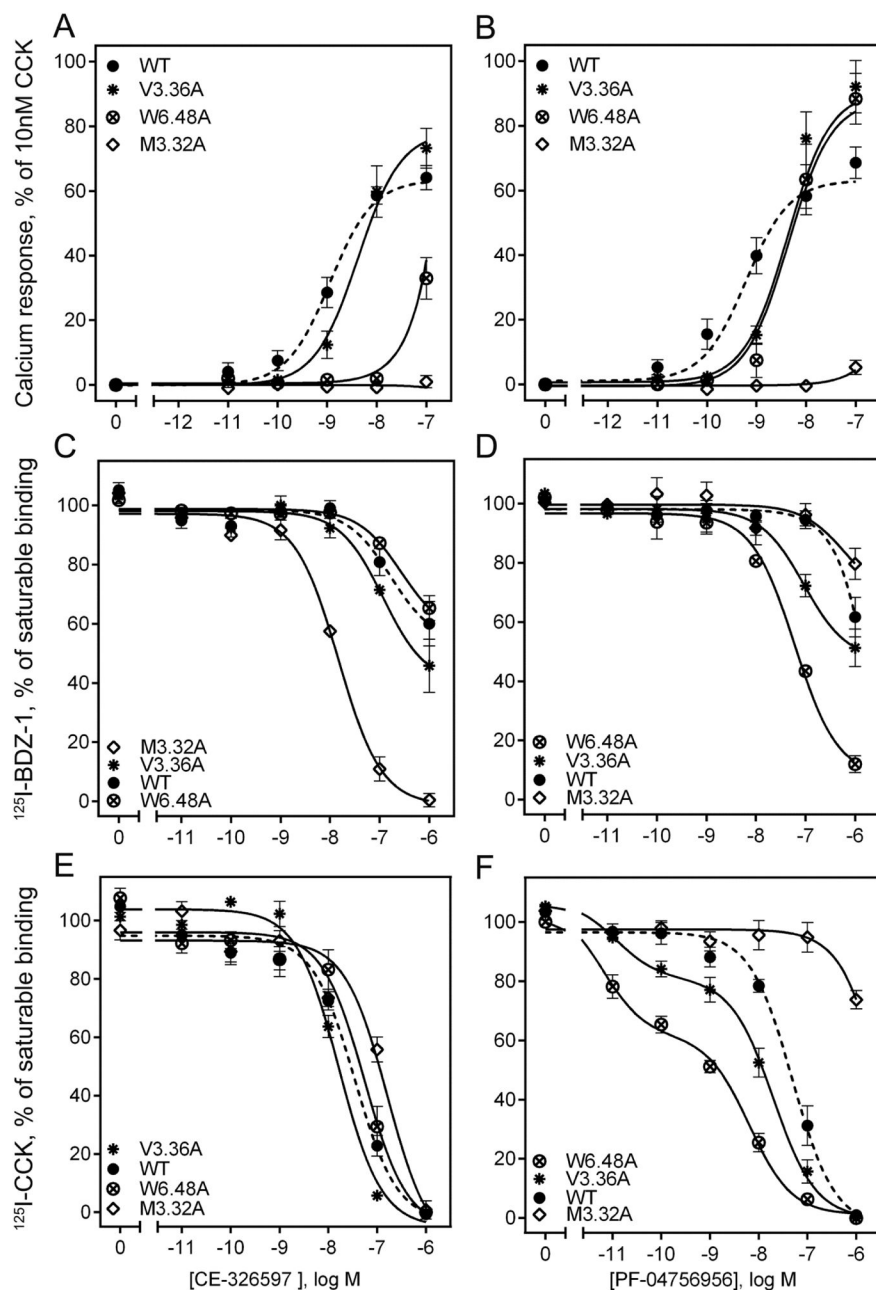


**Figure 9. Impact of selected receptor mutations on CE-326597 and PF-04756956 binding and biological activity**

Shown are the effects of alanine-replacement mutants of three residues predicted by the molecular models as potentially interacting with these small molecule agonists (CE-326597 in the left column and PF-04756956 in the right column). Biological activity data (stimulation of intracellular calcium responses) are shown in the top panels (A and B), while competition-binding data are shown in the middle row for the benzodiazepine radioligand (panels C and D) and in the bottom row for the CCK-like peptide radioligand (panels E and F). The X-axis values reflect the absence of ligand (0) to the left of the break, and log molar

concentrations to the right of the break. Data are expressed as means  $\pm$  S.E.M. of duplicate determinations from four to six independent experiments.

Author Manuscript

Author Manuscript

Author Manuscript

Author Manuscript

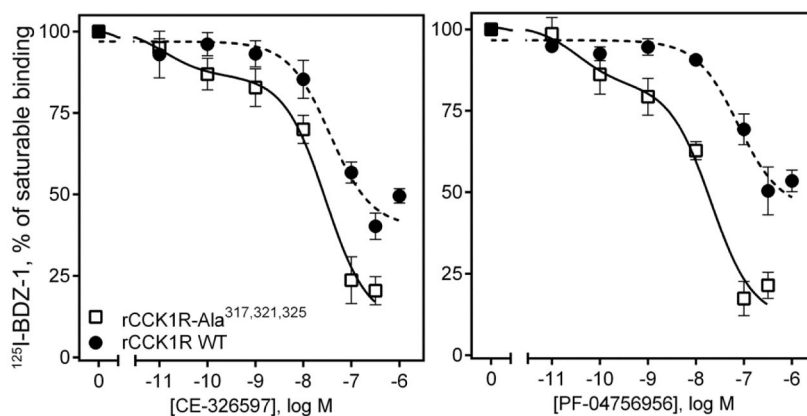


**Figure 10. Ligand binding at wild type (dimerizing) and non-dimerizing mutant of CCK1R** Shown is the ability of CE-326597 and PF-04756956 to inhibit saturable binding of  $^{125}\text{I}$ -BDZ-1 to wild type rat CCK1R and a non-dimerizing mutant of this receptor (rat CCK1R-Ala<sup>(317,321,325)</sup>) expressed in COS cells. The triazolobenzodiazepinones inhibited saturable binding of the BDZ radioligand in the non-dimerizing mutant construct to a greater degree than at wild type CCK1R. The X-axis values reflect the absence of ligand (0) to the left of the break, and log molar concentrations to the right of the break. Data are expressed as means  $\pm$  S.E.M. of duplicate determinations from three to five independent experiments.

Binding parameters for CE-326597 and PF-04756956 at wild type CCK receptors using the  $^{125}\text{I}$ -CCK and  $^{125}\text{I}$ -BDZ-1 (for CCK1R) or  $^{125}\text{I}$ -BDZ-2 (for CCK2R) radioligands, applying the competitive and allosteric ternary complex models.

Table 1

Radioligand Analysis type	$^{125}\text{I}$ -CCK				$^{125}\text{I}$ -BDZ-1/2				
	Competitive		Allosteric		Competitive		Allosteric		
	CCK1R WT	CCK2R WT	CCK1R WT	CCK2R WT	CCK1R WT	CCK2R WT	CCK1R WT	CCK2R WT	
CE-326597	pIC <sub>50</sub>	7.65 ± 0.04	6.56 ± 0.14##	—	—	6.21 ± 0.14	6.85 ± 0.13#	—	—
	pK <sub>i,fb</sub>	6.56 ± 0.18	>6.00#	7.61 ± 0.03**	7.15 ± 0.30***	6.37 ± 0.08	6.77 ± 0.07#	6.78 ± 0.14	7.61 ± 0.06***
	α	—	—	~0.00	0.32 ± 0.01#	—	—	0.54 ± 0.06	0.47 ± 0.06
PF-04756956	pIC <sub>50</sub>	7.56 ± 0.08	6.16 ± 0.14##	—	—	>6.00	>6.00	—	—
	pK <sub>i,fb</sub>	6.67 ± 0.10	5.85 ± 0.24#	7.54 ± 0.06**	6.67 ± 0.35##	>6.00	5.90 ± 0.12	6.04 ± 0.14	7.16 ± 0.26*##
	α	—	—	~0.0	0.32 ± 0.07#	—	—	0.65 ± 0.08	0.60 ± 0.04

\*# p < 0.05,

\*\*## p < 0.01.

\* denotes comparison with the corresponding K<sub>i</sub> value;

# denotes comparison with CCK1R.

**Table 2**

Biological activity of CE-326597 and PF-04756956 at CCK1R- or CCK2R-based chimeric receptor constructs.

CCK1R-based chimeric receptors	Receptor abbreviations	CE-326597, pEC <sub>50</sub>	PF-04756956, pEC <sub>50</sub>
CCK1R WT	CCK1R	8.82 ± 0.08	9.47 ± 0.08
N2.61T	CCK1R TM2	9.28 ± 0.07**	9.54 ± 0.05
T3.28V, T3.29S	CCK1R TM3	8.86 ± 0.07	9.92 ± 0.08**
I6.51V, F6.52Y	CCK1R TM6	7.38 ± 0.09**	7.16 ± 0.07**
L7.39H	CCK1R TM7	NR	>7.00**
CCK2R-based chimeric receptors	Receptor abbreviations	CE-326597, pEC <sub>50</sub>	PF-04756956, pEC <sub>50</sub>
CCK2R WT	CCK2R	6.01 ± 0.07	NR
T2.61N	CCK2R TM2	>6.00	NR
V3.28T, S3.29T	CCK2R TM3	>6.00	NR
V6.51I, Y6.52F	CCK2R TM6	6.55 ± 0.13*	>6.00*
H7.39L	CCK2R TM7	7.23 ± 0.13**	>6.00*

\* p < 0.05;

\*\* p < 0.01 compared with wild type CCK receptor

Table 3

Binding parameters of CE-326597 and PF-04756956 at CCK1R- or CCK2R-based chimeric receptor constructs.

CCK1R-based chimeric receptors	Receptor abbreviations	CE-326597, pIC <sub>50</sub>		PF-04756956, pIC <sub>50</sub>	
		<sup>125</sup> I-BDZ-1	<sup>125</sup> I-CCK	<sup>125</sup> I-BDZ-1	<sup>125</sup> I-CCK
CCK1R WT	CCK1R	6.21 ± 0.14	7.65 ± 0.04	>6.00	7.56 ± 0.08
N2.61T	CCK1R TM2	7.03 ± 0.10**	8.70 ± 0.12**	6.98 ± 0.18**	9.09 ± 0.14**
T3.28V, T3.29S	CCK1R TM3	8.35 ± 0.08**	7.43 ± 0.05	8.14 ± 0.08**	7.37 ± 0.03
I6.51V, F6.52Y	CCK1R TM6	6.00 ± 0.10	7.37 ± 0.12	6.00 ± 0.18	7.15 ± 0.10
L7.39H	CCK1R TM7	>6.00*	6.17 ± 0.12**	>6.00*	6.10 ± 0.10**
CCK2R-based chimeric receptors	Receptor abbreviations	CE-326597, pIC <sub>50</sub>		PF-04756956, pIC <sub>50</sub>	
CCK2R WT	CCK2R	<sup>125</sup> I-BDZ-2	<sup>125</sup> I-CCK	<sup>125</sup> I-BDZ-2	<sup>125</sup> I-CCK
T2.61N	CCK2R TM2	6.85 ± 0.13	6.56 ± 0.22	>6.00	6.16 ± 0.14
V3.28T, S3.29T	CCK2R TM3	NDB	>6.00**	NDB	>6.00**
V6.51I, Y6.52F	CCK2R TM6	>6.00*	6.68 ± 0.26	>6.00*	6.52 ± 0.17
H7.39L	CCK2R TM7	>6.00	8.77 ± 0.19**	>6.00	>6.00
		8.70 ± 0.21**	8.00 ± 0.11**	8.12 ± 0.21**	

\* p < 0.05;

\*\* p < 0.01 compared with wild type CCK receptor. NDB no detectable binding.



Table 4

Binding and biological activity parameters of CCK, CE-326597 and PF-04756956 at CCK1R-based mutants derived from the best fitting models.

CCK1R-based chimeric receptors	Receptor abbreviations	CCK, pIC <sub>50</sub>	CCK binding, F <sub>max</sub> (pmol/mg)	CE-326597, pIC <sub>50</sub>		PF-04756956, pIC <sub>50</sub>		CCK, pEC <sub>50</sub>	CE-326597, pEC <sub>50</sub>	PF-04756956, pEC <sub>50</sub>
				<sup>125</sup> I-BDZ-I	<sup>125</sup> I-CCK	<sup>125</sup> I-BDZ-I	<sup>125</sup> I-CCK			
CCK1R WT	CCK1R	8.93 ± 0.12	5.0 ± 1.0	6.29 ± 0.21	7.52 ± 0.04	>6.00	7.41 ± 0.10	10.66 ± 0.08	8.75 ± 0.08	9.38 ± 0.10
M3.32A	CCK1R M121A	7.78 ± 0.10 <sup>**</sup>	151 ± 63 <sup>**</sup>	7.82 ± 0.04 <sup>**</sup>	6.78 ± 0.09 <sup>**</sup>	>6.00	>6.00 <sup>**</sup>	9.89 ± 0.05 <sup>**</sup>	NR	NR
V3.36A	CCK1R V125A	9.86 ± 0.21 <sup>*</sup>	0.9 ± 0.4 <sup>*</sup>	6.10 ± 0.19	7.78 ± 0.04	6.02 ± 0.11	8.00 ± 0.16 <sup>*</sup>	10.32 ± 0.10 <sup>*</sup>	8.51 ± 0.03 <sup>**</sup>	8.48 ± 0.03 <sup>**</sup>
W6.48A	CCK1R W326A	9.33 ± 0.18	0.8 ± 0.2 <sup>*</sup>	6.57 ± 0.21	7.38 ± 0.07	7.21 ± 0.08 <sup>**</sup>	8.85 ± 0.05 <sup>**</sup>	10.36 ± 0.06 <sup>*</sup>	>7.00 <sup>**</sup>	8.30 ± 0.11 <sup>**</sup>

\* p < 0.05;

\*\* p < 0.01 compared with wild type CCK1 receptor. NR, no detectable response.